

## HNPS Advances in Nuclear Physics

Vol 12 (2003)

HNPS2003



### Multipole Response of Ni and Sn Isotopes and its Momentum Dependence

*P. Papakonstantinou, E. Mavrommatis, J. Wambach, V. Yu. Ponomarev*

doi: [10.12681/hnps.3350](https://doi.org/10.12681/hnps.3350)

#### To cite this article:

Papakonstantinou, P., Mavrommatis, E., Wambach, J., & Ponomarev, V. Y. (2021). Multipole Response of Ni and Sn Isotopes and its Momentum Dependence. *HNPS Advances in Nuclear Physics*, 12, 110–117. <https://doi.org/10.12681/hnps.3350>

# Multipole response of Ni and Sn isotopes and its momentum dependence

P. Papakonstantinou<sup>a</sup> E. Mavrommatis<sup>a</sup> J. Wambach<sup>b</sup>  
V.Yu. Ponomarev<sup>b</sup>

<sup>a</sup>*Physics Department, Nuclear and Particle Physics Section, University of Athens,  
GR-15771 Athens, Greece*

<sup>b</sup>*Institute für Kernphysik, Technische Universität Darmstadt, Schlossgartenstr.9,  
D-64289 Darmstadt, Germany*

---

## Abstract

We have used a self-consistent Skyrme-HF plus Continuum RPA model to study the low-multipole response of stable and neutron/proton-rich Ni and Sn isotopes. We focus on the momentum dependence of the strength distribution, as it may provide information on the structure of excited nuclear states.

---

## 1 Introduction

The theoretical and experimental study of nuclei close to the drip lines is currently in progress, aiming to illuminate the effect of the excess proton or neutron number on the nuclear response and in particular on giant resonances (see for example the contributions in [1,2,3]). We have used a self-consistent Skyrme-Hartree-Fock plus Continuum RPA model to examine the low-multipole response of stable and neutron/proton-rich Ni and Sn isotopes. Experimental studies of these nuclei are being planned at RIKEN [4]. In this work, we focus on the momentum dependence of the strength distribution. The motivation for pursuing this can be summarized as follows:

- Theoretically, the transition density associated with a particular type of excitation approaches hydrodynamical behaviour in the case of very collective states, such as giant resonances, but in general it is expected to be energy dependent.
- It is important to have a reliable microscopic description of the transition density characterizing a nuclear excitation not only to gain insight on the nature of the excitation but also because theoretical transition densities

enter the analysis of electron- or hadron-scattering experiments aiming at identifying giant resonances. Macroscopic descriptions may be inadequate in certain cases.

- The question arises as to whether the giant resonances, and in general the multipole response, of drip-line nuclei differ significantly from the ones of stable nuclei. Interesting theoretical predictions, which are worth examining further in terms of the transition density, include the increased fragmentation of giant resonances in the case of drip-line nuclei and the occurrence of the so-called threshold strength, namely a significant amount of strength just above the neutron threshold and below the energy region of the giant resonance, in the case of neutron-rich nuclei.
- It is possible to study the momentum dependence of nuclear response experimentally using inelastic electron scattering.

The RPA method describes satisfactorily the transition densities of collective states in stable nuclei. The RPA has also been used in the past to study transition densities of individual excitations in the case of unstable nuclei and to compare with the behaviour of stable nuclei [5,6,7,8,9,10,11]. In this work we follow an alternative -and, in principle, equivalent- approach which allows a more systematic study. We will examine how the transition strength distribution varies with the momentum  $q$  transferred to the system. For this we consider an external field of the form  $j_L(qr)$ .

## 2 Definitions and method of calculation

We consider the response of spherical, closed-(sub)shell nuclei to an external field of the type  $V_{L0} = \sum_{i=1}^A V_L(r_i, t_i) Y_{L0}(\theta_i, \phi_i)$ , where the variable  $t_i = p$  or  $n$  labels the isospin character -proton or neutron- of the  $i$ -th particle. For an isoscalar (IS) field,  $V_L(r, p) = V_L(r, n) \equiv V_L(r)$  and for an isovector (IV) one  $V_L(r, p) = -V_L(r, n) \equiv V_L(r)$ . For  $L = 1$  we use an effective charge equal to  $-\frac{2N}{A}$  for protons and  $\frac{2Z}{A}$  for neutrons. In the following, the isospin label will be suppressed for the sake of simplicity.

We set  $V_L(r) = [4\pi(2L+1)]^{1/2} j_L(qr)$ , where  $j_L$  is a spherical Bessel function. In the long-wavelength limit  $qR \rightarrow 0$  ( $R$  is the nuclear radius), we obtain the usual multipole operator of the form  $r^L$  for  $L > 0$  and  $r^2$  for  $L = 0$ . The IS transition density  $\delta\rho_{L0}(\vec{r})$  characterizing the excited natural-parity state  $|L0\rangle$  of energy  $E$ , is determined by its radial component  $\delta\rho_L(r)$ , where

$$\delta\rho_{L0}(\vec{r}) = (2L+1)^{-1/2} \delta\rho_L(r) Y_{L0}(\theta, \phi). \quad (1)$$

The strength distribution  $S(E) = \sum_f \langle 0 | V_{L0} | f \rangle^2 \delta(E - E_f)$  (where  $|f\rangle$  are the final states excited by the external field  $V_{L0}$  and  $E_f$  their excitation energies)

is related to the Fourier transform of  $\delta\rho_L(r)$ . In particular, since we are dealing with continuous distributions, we write the strength in a small energy interval of width  $\Delta E$  at energy  $E$  as

$$\begin{aligned} S(E) &= \frac{4\pi(2L+1)}{\Delta E} \left| \int_0^\infty dr \delta\rho_L(r) j_L(qr) r^2 \right|^2 \\ &= \frac{(2L+1)}{\Delta E} \left| \int d^3r \delta\rho_{L0}(\vec{r}) e^{i\vec{q}\cdot\vec{r}} \right|^2 \propto |F_L(q^2)|^2. \end{aligned} \quad (2)$$

The quantities introduced above are calculated using a Skyrme - Hartree-Fock (HF) plus Continuum - RPA (CRPA) model. For the HF ground-state, the numerical code of P.-G. Reinhard [12] is used. The calculation of the response function (unperturbed HF, as well as RPA) is formulated in coordinate space, as described in [13,14,15,16,17]. The radial part of the unperturbed  $ph$  Green function, of multipolarity  $L$ , is given by:

$$G_L^0(r, r'; E) = \sum_{ph} \left\{ \frac{\langle p || O_L || h \rangle_r^* \langle p || O'_L || h \rangle_{r'}}{\varepsilon_{ph} - E} \pm \frac{\langle h || O'_L || p \rangle_{r'}^* \langle h || O_L || p \rangle_r}{\varepsilon_{ph} + E} \right\}, \quad (3)$$

where  $O_L$  (or  $O'_L$ ) is one of the operators  $Y_{L0}$ ,  $[Y_L \otimes (\nabla^2 + \nabla'^2)]_{L0}$ ,  $[Y_{L\pm 1} \otimes (\vec{\nabla} - \vec{\nabla}')]_{L0}$  and  $[Y_{L\pm 1} \otimes (\vec{\nabla} + \vec{\nabla}')]_{L0}$ . The sign of the second term depends on the symmetry properties of the operators  $O_L$  and  $O'_L$  under parity and time-reversal transformations. Spin operators have been omitted in the present calculation. With  $h$  ( $p$ ) we denote the quantum numbers of the HF hole(particle) state and  $\varepsilon_{ph} = \varepsilon_p - \varepsilon_h$  is the energy of the unperturbed  $ph$  excitation. The particle continuum is fully taken into account, as described in [13,16,18]. A small but finite  $\text{Im}E$  ensures that bound transitions acquire a finite width [13]. The RPA  $ph$  Green function is given by the equation

$$G_L^{\text{RPA}} = [1 + G_L^0 V_{\text{res}}]^{-1} G_L^0, \quad (4)$$

which is solved as a matrix equation in coordinate space, isospin character and operators  $O_L$ . The  $ph$  residual interaction  $V_{\text{res}}$  is zero-range, of the Skyrme type, derived self-consistently from the Skyrme-HF energy functional [16,19]. From the Green function  $G_L^{\text{RPA}}$  for  $O_L = O'_L = Y_L$  the strength distribution  $S(E)$  is obtained,

$$S(E) = 4(2L+1) \text{Im} \int j_L(qr) G_L^{\text{RPA}}(r, r') j_L(qr') dr dr'. \quad (5)$$

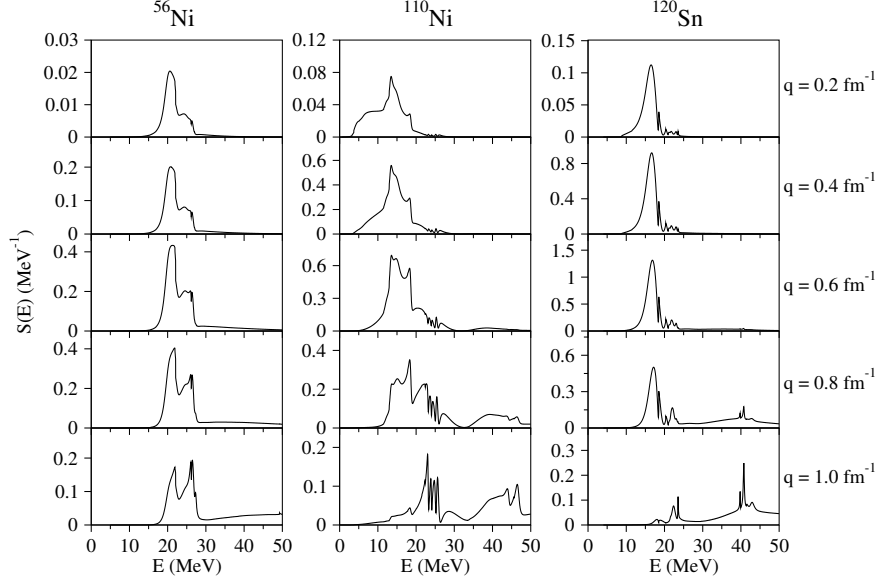


Figure 1. ISM strength distribution as a function of energy and momentum transfer.

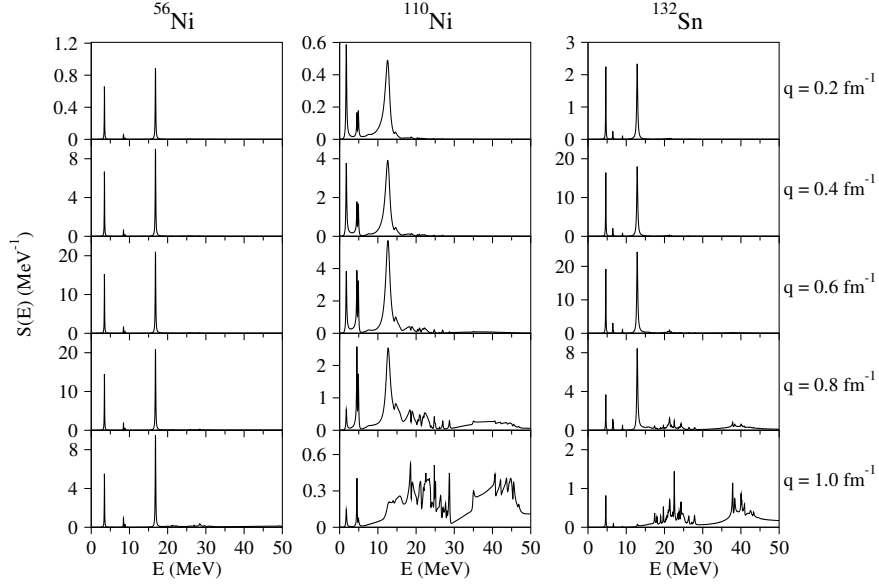


Figure 2. ISQ strength distribution as a function of energy and momentum transfer.

### 3 Results

We have calculated the IS and IV monopole (ISM and IVM), IV dipole (IVD) and IS and IV quadrupole (ISQ and IVQ) response of the nuclei  $^{56,78,110}\text{Ni}$  and  $^{110,120,132}\text{Sn}$  using the RPA method described above and the Skyrme parametrization SkM\*, for  $q = 0.2, 0.4, 0.6, 0.8, 1.0 \text{ fm}^{-1}$ . Selected results are presented in Figs. 1-5. Next we comment on these results.

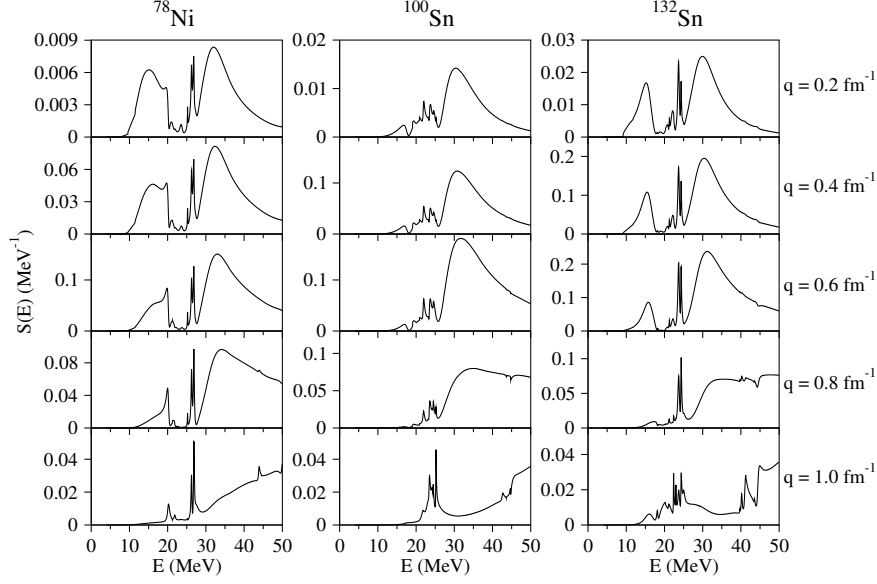


Figure 3. IVM strength distribution as a function of energy and momentum transfer.

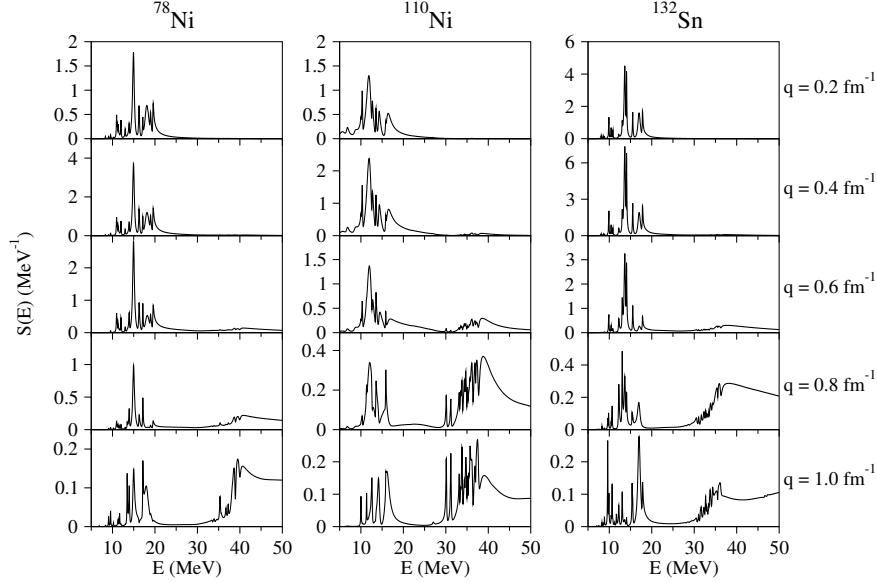


Figure 4. IVD strength distribution as a function of energy and momentum transfer.

**Strength is shifted to higher energies** In all cases, as  $q$  increases, the strength distribution is shifted to higher energies, which can be interpreted as the onset of the quasielastic peak. Also, overtones of giant resonances become visible. For instance, in the ISM response, Fig. 1, strength is shifted from the  $2\hbar\omega$  region to the  $4\hbar\omega$  region. In the IVD response, Fig. 4, strength is found in the  $3\hbar\omega$  region as  $q$  increases. Excitations of single-particle character, with density oscillations taking place in the interior of the nucleus, give rise to this behaviour of the form factor. In the light nucleus  $^{56}\text{Ni}$  the shift takes place more slowly as a function of  $q$  than in heavier nuclei, such as  $^{120}\text{Sn}$ .

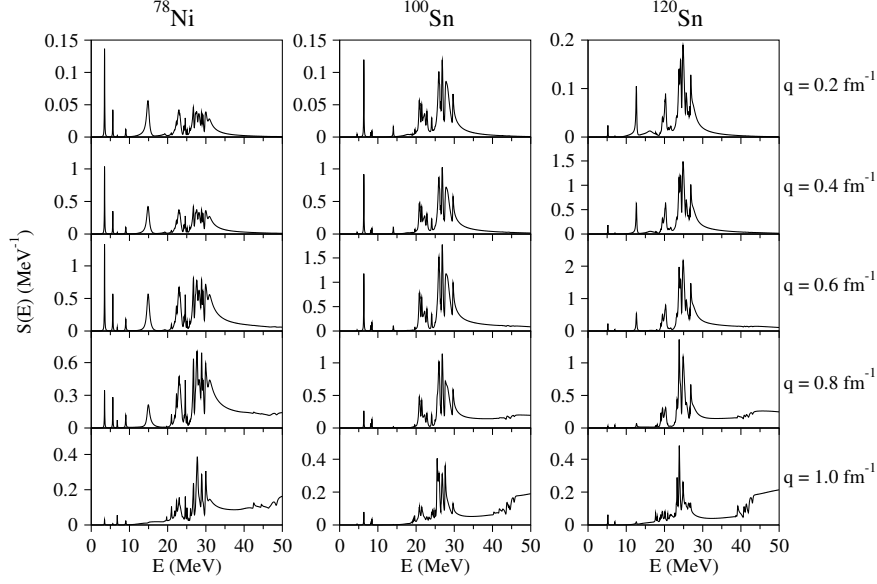


Figure 5. IVQ strength distribution as a function of energy and momentum transfer.

**Threshold strength** In the case of neutron-rich nuclei the threshold strength (TS) vanishes rapidly as  $q$  increases. This is seen clearly in the case of  $^{110}\text{Ni}$ . As we observe in Fig. 1 (right panel, RP), the ISM TS behaves differently than the IS GMR which is located a few MeV higher in energy. The same holds for the IVM response, Fig. 3 (RP), and similarly for the IVD, Fig. 4 (RP). A major role in this effect is played by the weakly bound neutrons outside the core, which are distributed at large distances from the nuclear center, resulting in form factors  $F_L(q)$  with maxima at lower values of  $q$ .

In Ref. [5] the ISM response of the neutron-rich nucleus  $^{60}\text{Ca}$  is examined - where a significant amount of TS appears as well. It was found that in the region of the GMR the transition density compares rather well with the Tassie model prediction, whereas in the TS region it is extended at large distances and it originates mostly from neutron excitations. A similar effect was predicted also in the case of the ISQ response of  $^{28}\text{O}$  [6].

**Isoscalar monopole response** In Fig. 1 the ISM response of  $^{56}\text{Ni}$ ,  $^{110}\text{Ni}$  and  $^{120}\text{Sn}$  is presented. We observe that the form factor of the fine structure just above the GMR of  $^{120}\text{Sn}$  is more flat, between  $q = 0.4 - 0.8 \text{ fm}^{-1}$ , compared to the GMR. The same holds for the other Sn isotopes and for  $^{78}\text{Ni}$  (not shown). The GMR width of the light nucleus  $^{56}\text{Ni}$  is large. In Fig. 1 two distinct energy regions can be recognized: the region  $P_<$  below  $\mathcal{E}_0 \approx 23 \text{ MeV}$ , and the region  $P_>$  above  $\mathcal{E}_0$ . According to macroscopic models, the GMR is a uniform compression mode whose transition density has a node at the nuclear surface. In the case of  $^{56}\text{Ni}$  the node would then occur at radius  $R \approx 4.6 \text{ fm}$ . Therefore, the transition density for  $q = q_{01} = \pi/R = 0.68 \text{ fm}^{-1}$  would show maximal overlap with the function  $j_0(qr)$  (whose 1st root equals  $\pi$ ). It seems that the

form factor in the region  $P_<$  follows this type of behaviour, since it reaches a maximum between 0.6 and 0.8 fm<sup>-1</sup>. The form factor in  $P_>$  is maximized at a larger value of  $q$  and therefore it does not correspond to such a collective behaviour.

**Isoscalar quadrupole response** The two peaks in the ISQ strength distribution of <sup>56</sup>Ni (see Fig. 2), <sup>78</sup>Ni (not shown) and <sup>100,120</sup>Sn (not shown), namely the low-lying collective transition and the IS GQR, show similar behaviour as a function of  $q$  up to  $q \approx 0.8$  fm<sup>-1</sup>. This is due to the fact that in these nuclei, the transition density of both states is peaked at the surface. In the case of <sup>132</sup>Sn, Fig. 2, the form factor of the first peak does not follow the behaviour of the GQR form factor. In <sup>110</sup>Ni, Fig. 2, there is a clear difference. The low-energy peak loses its strength faster than the GQR, behaving like the threshold strength of other multipolarities. This effect is attributed to the excessive loosely bound neutrons outside the core, resulting in transition densities peaking beyond the surface of the core. In <sup>110</sup>Ni a third peak occurs between the low-lying state and the GQR, also showing different behaviour. It peaks at higher  $q$  than the GQR and the low-lying state do. It is a non-collective state with a transition density localized in the interior of the nucleus. Such a peak occurs also in the case of <sup>78</sup>Ni (not shown).

**Isvector strength distributions** With the exception of the threshold strength in very-neutron-rich nuclei, the IVM strength distributions, Fig. 3, for  $q = 0.2, 0.4$  and  $0.6$  fm<sup>-1</sup> are similar to each other. The same seems to hold for the IVQ distributions, Fig. 5, in the region of the IV GQR, in spite of the rich structure of the latter, and, to a lesser extent, in the case of the IVD distributions, Fig. 4.

## 4 Conclusion

According to our results, the transition density may show considerable energy dependence in the region of the IS GMR. The form factor of the threshold strength in very-neutron-rich nuclei, is narrower compared with the form factor of the respective giant resonance. This result is independent of  $L$ . In the region of IV GMR and GQR resonances, no significant energy dependence is observed for the low values of  $q$  examined here.



## References

- [1] Proc. Topical Conference on Giant Resonances, Varenna, May 11-16 1998. *Nucl. Phys.* **A649** (1999).
- [2] Proc. International Conference on Giant Resonances, Osaka, June 12-15, 2000. *Nucl. Phys.* **A687** (2001).
- [3] Proc. COMEX1, Int. Conference on Conference on Collective Motion under Extreme Conditions, Paris, June 10-13, 2003, to be published in *Nucl. Phys.* **A**.
- [4] RI Beam Factory Documentation. *Basic Science*, 1998. <http://riksun.riken.go.jp/ribf/doc>.
- [5] I. Hamamoto, H. Sagawa, and X.Z. Zhang. *Phys. Rev.* **C56** (1997) 3121.
- [6] I. Hamamoto and H. Sagawa. *Phys. Rev.* **C54** (1996) 2369.
- [7] I. Hamamoto, H. Sagawa, and X.Z. Zhang. *Phys. Rev.* **C53** (1996) 765.
- [8] I. Hamamoto, H. Sagawa, and X.Z. Zhang. *Phys. Rev.* **C55** (1997) 2361.
- [9] F. Catara, E.G. Lanza, M.A. Nagarajan, and A. Vitturi. *Nucl. Phys.* **A614** (1997) 86.
- [10] F. Catara, E.G. Lanza, M.A. Nagarajan, and A. Vitturi. *Nucl. Phys.* **A624** (1997) 449.
- [11] S. Kamezdzhev, J. Speth, and G. Tertychny. *Nucl. Phys.* **A624** (1997) 328.
- [12] P.-G. Reinhard. Skyrme-Hartree-Fock Model. *in Computational Nuclear Physics I - Nuclear Structure*, ed. K. Langanke, J.E. Maruhn and S.E. Koonin (Springer, New York 1991) p.28.
- [13] G. Bertsch. The random phase approximation for collective excitations. *in Computational Nuclear Physics I - Nuclear Structure*, ed. K. Langanke, J.E. Maruhn and S.E. Koonin (Springer, New York 1991) p.75.
- [14] G.F. Bertsch and S.F. Tsai. *Phys. Rep.* **18C** (1975) 127.
- [15] N. Van Giai and H. Sagawa. *Nucl. Phys.* **A371** (1981) 1.
- [16] Nguyen Van Giai. *Nuclear Collective Dynamics*, page 356. World Scientific, 1983.
- [17] J. Ryckebusch. Ph.d. thesis, University of Gent, 1988.
- [18] S. Shlomo and G.F. Bertsch. *Nucl. Phys.* **A243** (1975) 507.
- [19] S.F. Tsai. *Phys. Rev.* **C17** (1978) 1862.